CRYSTAL GROWTH & DESIGN

Article

Cite This: *Cryst. Growth Des.* 2018, 18, 5663−5673

pubs.acs.org/crystal

# Calcium Carbonate Crystal Shapes Mediated by Intramineral Proteins from Eggshells of Ratite Birds and Crocodiles. Implications to the Eggshell's Formation of a Dinosaur of 70 Million Years Old

Angélica Legorreta-Flores,[†] Alejandra Davila-Tejeda,[†,‡] Omar Velásquez-González,[†,‡] Eduardo Ortega,[§] Arturo Ponce,[§] Hiram Castillo-Michel,[∥] Juan Pablo Reyes-Grajeda,[⊥] Rene Hernández-Rivera,[#] Mayra Cuéllar-Cruz,[▽] and Abel Moreno*[,†]

[†]Instituto de Química and [#]Instituto de Geología, Universidad Nacional Autónoma de México, Av. Universidad 3000, Cd.Mx. 04510, México

[‡]Escuela de Química & Escuela de Química Farmacéutica, Universidad de San Carlos Guatemala, Ciudad de Guatemala, Guatemala

[§]Department of Physics and Astronomy, University of Texas at San Antonio, One UTSA Circle, San Antonio, Texas 78249, United States

[∥]European Synchrotron Radiation Facility, B.P. 220 Grenoble, France

[⊥]Instituto Nacional de Medicina Genómica, Ciudad de México, CDMX, México

[▽]Departamento de Biología, División de Ciencias Naturales y Exactas, Campus Guanajuato, Universidad de Guanajuato, Noria Alta S/N, Col. Noria Alta, C.P. 36050 Guanajuato, Guanajuato, México

*Web-Enhanced Feature* *Supporting Information*

**ABSTRACT:** In this contribution we want to show how the intramineral proteins affect the crystal morphology of calcite crystals grown in vitro. Intramineral proteins from emu eggshells and two crocodile species were isolated, purified by ultrafast liquid chromatography, and characterized by biochemical and biophysical methods. We saw that the crystal habit of calcite was modified when intramineral proteins were present at certain concentration. Therefore, all crystal species were individually characterized by scanning electron microscopy (SEM) and by electron diffraction with an electron-reduced dosage in transmission electron microscopy. Additionally, transversal SEM micrographs of eggshells of four types of species, namely, emu, crocodile, hen, and dinosaur (70 million years old), were compared to track the changes produced by the interacting intramineral proteins. Finally, the organic sulfur content analysis of these eggshells was performed by using X-ray absorption techniques like X-ray fluorescence and X-ray absorption near-edge structure. From the analyses of the dinosaur eggshells, these X-ray absorption data showed a very characteristic organic sulfur bonding similar to that semiessential proteogenic amino acid L-cysteine, which implies that there is a possibility of having a very old intramineral protein similar to those found in emu and crocodiles.

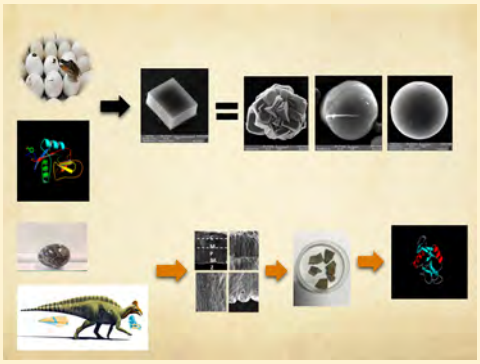

## 1. INTRODUCTION

Biomineralization is related to the study of the formation, the structure−function relationship, and physicochemical properties of inorganic solids deposited in biological systems. These mineralization processes have important implications for evolution,[1] environmental sciences,[2] biomedical[3] and biological approaches,[4] and materials science connected to other scientific areas.[5] Particularly, the biomineralization of calcium salts in nature plays a major role in the understanding of the origin of life, as well as the processes of formation of biominerals in bone, teeth and shells, etc.[6] Over half of the chemical elements, essential for life, are incorporated as biominerals in humans. Some deposits, and particularly calcium carbonate, are distinguished not only for being widespread but also for being the most common constituent of a variety of shells in nature.[7] From those shells, the formation of eggshells in birds is the most intriguing biological system to be studied, not only due to the variety of eggshell shapes, mechanical properties, and structures but also to the way in which some specific intramineral proteins are involved in the nucleation control and crystal growth of calcium carbonate crystallites.[8] However, only a very few intramineral proteins have been crystallized and obtained in a crystallographic three-dimensional (3D) structure. The ovocleidin-17 (OC-17) from *Gallus gallus* was the first intramineral protein isolated and crystallographically solved by X-ray diffraction

**Received:** July 5, 2018
**Revised:** August 7, 2018
**Published:** August 9, 2018






DOI: 10.1021/acs.cgd.8b01020
*Cryst. Growth Des.* 2018, 18, 5663−5673

techniques.[9] The second protein isolated from the ostrich (*Struthio camelus*) eggshells took a long time to be solved by X-ray crystallographic methods due to complicated biochemical strategies needed to separate the intramineral proteins, which usually exist in pairs inside the intramineral part of the eggshell.[10,11] The small differences in the loops for the intramineral proteins located in the nonstructured parts of the tertiary structure of the proteins make those proteins difficult to crystallize (intrinsically disordered zones). Additionally, there is a lack of structures of intramineral proteins available in the protein databank. Only a few of them have been sequenced to get the 3D crystallographic structures via X-ray crystallography.[12]

When comparing the eggshells of the bird of the superorder Palaeognathae (*S. camelus*, *Rhea americana*, and *D. novaehollandiae*) with the eggshells of the *G. gallus*, we found that the Palaeognathae's eggshells have two intraminerals proteins, whereas the *G. gallus* eggshells have only one. However, when investigating the eggshells of crocodiles, we found that they also have two main proteins, which implies that the crocodiles will also need to be classified as members of the Palaeognathae.[13] There is a lack of investigations about the mechanisms of the eggshell formation of the mentioned species of birds and nothing about reptiles based on crystallographic approaches.[14] According to the phylogenetic viewpoint from the dinosaurs to the ratite birds, the crocodiles are between both classes of the evolutionary phylogenetic tree. The intramineral proteins of these semiaquatic reptiles have never been studied, and these proteins could be closely related to the intramineral proteins of the ratite birds. This is because its phylogeny has similarities in their genetic characteristics.

There are essential elements in the process of biomineralization, particularly that of sulfur (S), which is not only essential in living organisms but also in the biological macromolecules forming disulfide bridges conferring stability to enzymes. Sulfur is usually found as thiol (R−SH) from cysteine residues; this is one of the most reactive species. Nonetheless, in biological systems the sulfur presents several oxidation states ranging from −2 to +6. When the thiol group of the cysteine is oxidized, this thiol is chemically transformed into four groups: disulfide bridge (−S−S−), sulfenic acid (cysteine-SOH), and the irreversible sulfinic (cysteine-$SO_2H$) and sulfonic (cysteine-$SO_3H$) groups.[15] X-ray absorption methods like $\mu$-XANES chemical imaging is usually applied for mapping the organic matrices containing SH/S−S groups.[16] All the eggshells of the ratite birds, crocodiles, and dinosaurs underwent this procedure.

The aim of this contribution is to investigate the influence of intramineral proteins (from the eggshells of one ratite bird (emu) and two species of crocodiles, isolated and purified) on the crystal habit modifications of calcium carbonate crystals grown in vitro. The analyses of the changes in the habit of these crystals were performed through scanning electron microscopy (SEM). To characterize the type of polymorph present in the synthesis of $CaCO_3$ in the presence of intramineral proteins, all crystals were individually characterized by electron diffraction with electron-reduced dosage in transmission electron microscopy (TEM). In the final part, the analysis of these eggshells by using X-ray absorption techniques was performed at the synchrotron facilities in terms of investigating the organic sulfur bonding contents. These sulfur contents were compared to the eggshells of a dinosaur. From the analyses of the dinosaur eggshells, these X-ray absorption methods showed a very characteristic organic sulfur bonding similar to that semiessential proteogenic amino acid L-cysteine, which implies that there is a possibility of having a very old intramineral protein (occluded into the mineralized eggshell) similar to those intramineral proteins found in emu and crocodiles.

## 2. EXPERIMENTAL SECTION

**2.1. Isolation, Purification, and Biochemical Characterization of Intramineral Proteins.** The proteins dromaiocalcins (DCA-1 and DCA-2) from emu (*Dromaius novahollandiae*) and crococalcins (CCA-M and CCA-A) from two species of crocodiles: *Crocodylus moreletii* (Mexican crocodile) and *Crocodylus acutus* (American crocodile) were isolated and purified as previously described by Mann and Siedler,[12] performing some modifications and optimization on the biochemical strategies as described by Ruiz-Arellano and Moreno.[17] The protein solution was concentrated by cryo-cooling method, and the extract was cryo-concentrated in Falcon tubes according to the methodology published recently[18] replacing the classic Amicon system of filtration/concentration. The sample was dialyzed according to the protocol already published by our group.[17] In the purification of all the intramineral proteins we used a Shodex SUS 316 column in a gel permeation chromatography. All protein injections were of 500 $\mu$L using a mobile phase acetate buffer at pH 5.0. The next step was to perform a reverse-phase chromatography with a C18 column. Each of the proteins had a final yield of ∼3 mg/mL. Since protein crystallization needed higher protein concentration, the protein solution had to be concentrated to 5 mg/mL by using classical Amicon filtration procedure (Millipore). The concentration in each of the steps along the purification process was performed by a Nanodrop spectrometer. The purified proteins were also characterized by sodium dodecyl sulfate−polyacrylamide gel electrophoresis (SDS-PAGE).

**2.2. Determination of the Isoelectric Point.** The isoelectric point was estimated by using two-dimensional (2D) gel isoelectrofocusing technique.[19] The results for DCA-1 and DCA-2 were 6.8 and 5.3, respectively. These are approximately the same values as those reported for these two proteins (6.4 and 4.48). In both cases there is an acidic isoelectric point value. In the particular case of proteins of the crocodile, CCA-1 showed an isoelectric point of 5.2, while CCA-2 showed 5.9. These results are in a good agreement with published results, where these acidic proteins are adequate for $CaCO_3$ interactions.[20]

**2.3. Protein Identification by Liquid Chromatography and Mass Spectroscopy LC-MS/MS.** A Bruker Esquire mass spectroscope was used to obtain the mass spectroscopy (MS) results using the matrix-assisted laser desorption/ionization (MALDI) technique. Since the intramineral proteins CCA-1 and CCA-2 have not been either sequenced or identified, we performed a protein identification by liquid chromatography (LC) coupled to Mass Espectroscopy LC-MS/MS equipment with an automatic sampler Finnigan MicroAS with a pump MS Surveyor coupled to LTQ Orbitrap. The chromatographic column was a C18 packed with silica. The buffers consisted of (a) 2% (v/v) formic acid and (b) 2% (v/v) formic acid and acetonitrile 100%. The column was charged with peptides keeping a flux rate of 600 nL/min. The solvent B increased from 2 to 35% in 18 min and then from 35 to 80% in 7 min. The data of LC-MS/MS were collected using the top12 depending data method combined with a dynamic exclusion of 7 s.

**2.4. Crystal Growth Assays for Calcium Carbonate.** The experiments for the crystallization of calcium carbonate were performed using a mushroom device from Triana Sci and Tech.[14] Ammonium carbonate was put on the reservoir to produce a homogeneous vapor pressure to alkalinize the droplets of final volume of 4 $\mu$L. $CaCl_2$ droplets (0.1 M) and protein droplets were put on the top of the device on the surface of carbon circles as shown in Figure 1. Protein solutions were added 1:1 (at 100, 250, or 500 $\mu$g/mL). All controls were prepared in the same way, though proteins were not included. The experiments were performed at 18 °C. For the TEM



DOI: 10.1021/acs.cgd.8b01020
Cryst. Growth Des. 2018, 18, 5663−5673

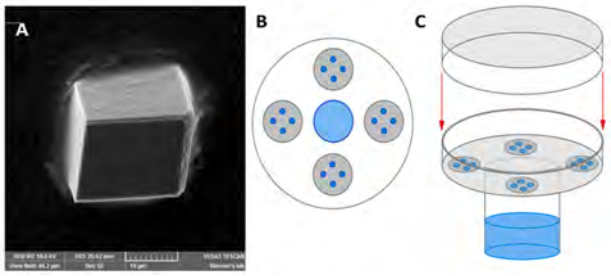


**Figure 1.** Experimental setup for the crystallization of calcium carbonate. (A) Control crystal of calcite. (B) The blue spots represent the droplets where the crystals were grown on the surface of the carbon circles. (C) The crystal growth device called "mushroom".

and electron diffraction experiments, the droplets were deposited on the surface of the copper grids to get those crystals ready for electron diffraction experiments. The concentrations of calcium chloride, ammonium carbonate, and all intramineral proteins were the same as those experimental setups for SEM. After the crystallization experiments were finished, the grids were carefully cleaned flushing those with deionized water. The grids were carefully cleaned (putting on edge those grids) with planar special tweezers (similar to those used for SEM). Then the grids were protected and attached to a plastic envelop to be sent to the TEM analysis.

**2.5. SEM, TEM, and Electron Diffraction Microscopies Applied to the Characterization of Calcium Carbonate Crystals.** $CaCO_3$ crystals were observed by SEM using a TESCAN VEGA3 SB microscope. Crystals were grown on a carbon circular tape, with afterward a sputtering system depositing a gold layer on the samples to improve the conductivity. The voltage to perform these analyses ranged from 10 to 20 kV for all measurements. TEM was performed in a field emission microscope model JEOL-2010F using 200 kV as accelerating voltage, and micrographs were collected in a highly sensitive CMOS camera. Electron diffraction patterns of individual calcium carbonate single crystals/formations were acquired under selected area electron diffraction (SAED) settings. To reduce radiation damage and preserve structural details, a combination of a small condenser aperture (30 $\mu$m), a highly excited condenser lens (8.06 V), a spread beam, and short time acquisition (0.5 s) was used to collect diffraction data in the order of ~200 e/Å$^2$. The electron diffraction patterns were indexed using electron microscopy simulation program.[21] Then after looking at coincidences in the patterns, the distances of the experimental planes were compared with the theoretical crystallographic planes to determine the phases for $CaCO_3$.

**2.6. Analyses of Protein Sequences by Multiple Alignment.** The multiple analyses of the sequence (MSA) of all homologous proteins was performed for OC-17, SCA-1, SCA-2, DCA-1, DCA-2, RCA-1, and RCA-2. These data were obtained from UniProt database in FASTA format. The alignment was initially performed by using ClustalW (EMBL-EBI). The phylogenetic tree of intramineral proteins was built based on the sequence of amino acids and using the algorithm Neighbor-joining using the version 3.5.0 of the program "R" and the phangorn library.

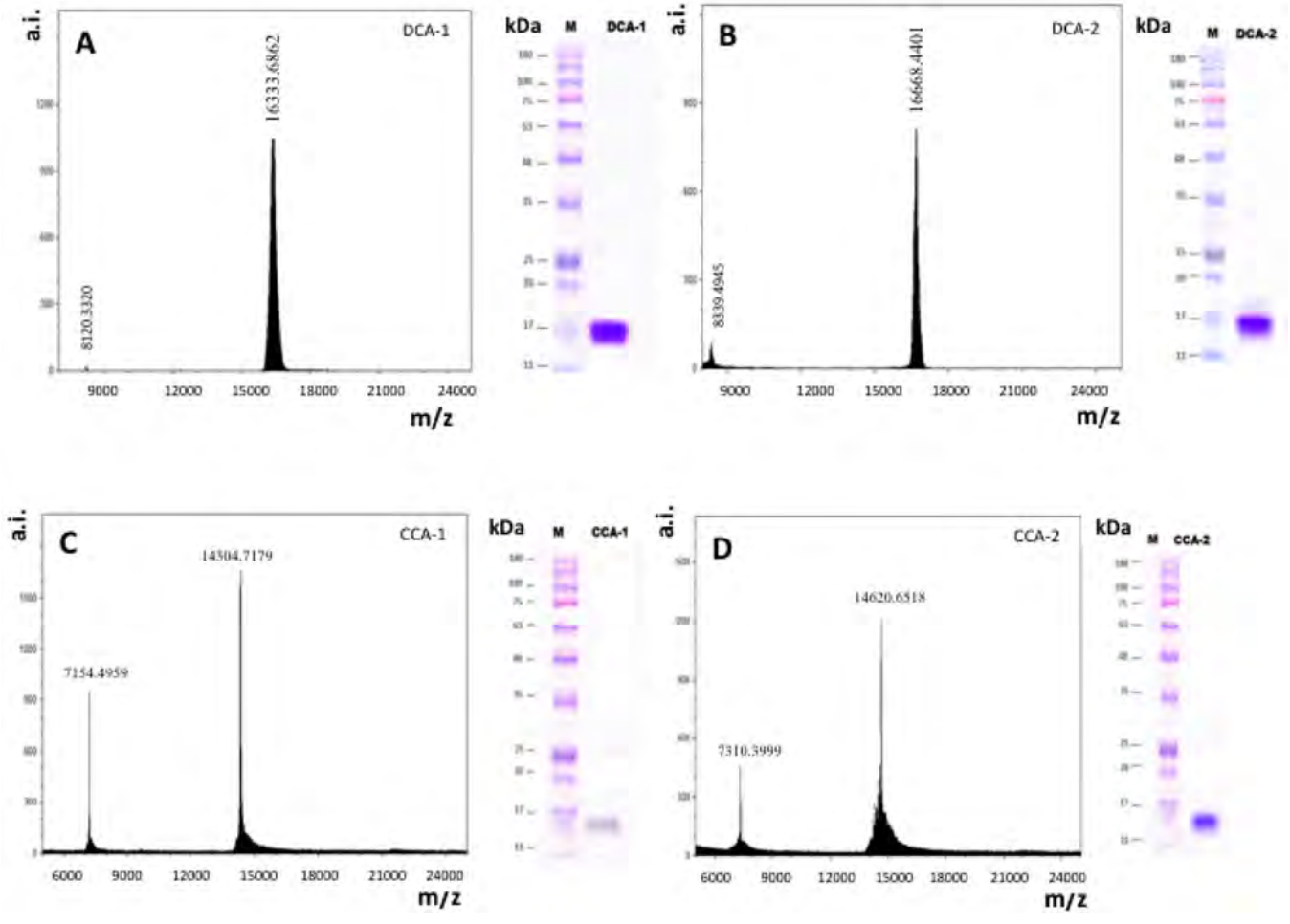


**Figure 2.** Spectra of (A) DCA-1, (B) DCA-2, (C) CCA-1, and (D) CCA-2. All of them were purified through molecular exclusion chromatography and were characterized by gel electrophoresis and mass spectroscopy.



DOI: 10.1021/acs.cgd.8b01020
Cryst. Growth Des. 2018, 18, 5663−5673

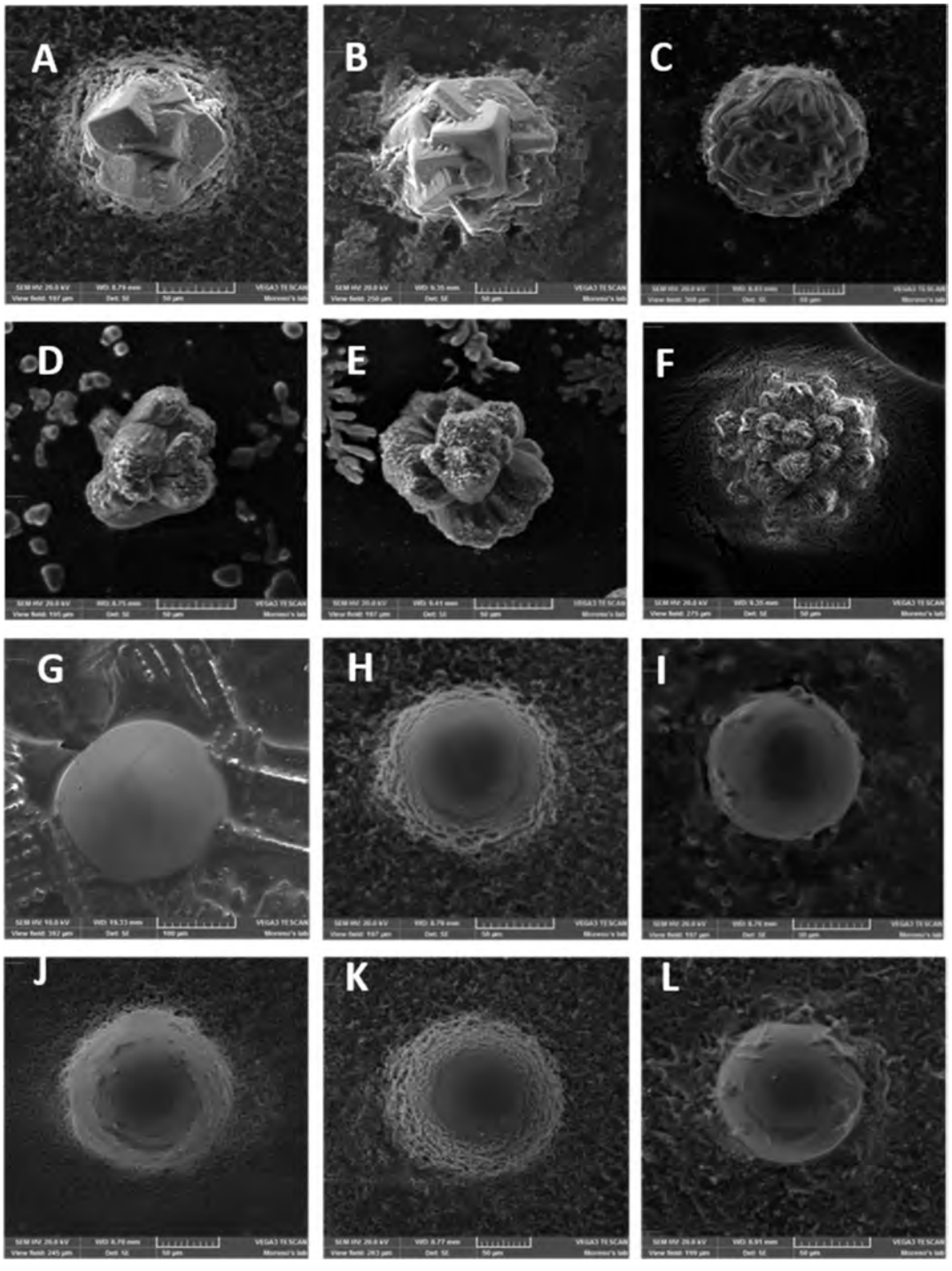


**Figure 3.** Crystallization of $CaCO_3$ in the presence of DCA1: (A) 100 $\mu$g/mL, (B) 250 $\mu$g/mL, (C) 500 $\mu$g/mL; (D−F) the same as previous, but including DCA-2, (G−I) using CCA-1 at different concentrations, and (J−L) $CaCO_3$ in the presence of CCA-2 at the same concentrations as those in (A−C).

**2.7. Characterization of Eggshells and Sulfur Chemical-Bonding via Synchrotron Microfocused X-ray Fluorescence and X-ray Absorption Near-Edge Spectroscopy.** Microfocused X-ray fluorescence ($\mu$-XRF) and microfocused X-ray absorption near-edge spectroscopy ($\mu$-XANES) were performed to analyze the sulfur distribution and speciation in modern and fossil eggshell samples. Energy selection was performed with the use of a Si (111) double crystal monochromator. Energy calibration was performed using $ZnS0_4$ and positioning the maximum absorbance feature at 2482.6 eV. The beam was focused using a Ni-coated fixed curvature KB mirror pair to a size of 0.8 × 0.3 $\mu m^2$. The flux at the sample was 1 × $10^{10}$ photons per second. Specific energies were selected to map S species with characteristic absorptions for disulfide organic (2473.4 eV), sulfate (2482.6 eV), and total S (2500 eV).[15] $\mu$-XRF maps were obtained at these energies by raster scanning the samples with step size ranging from 1 to 3 $\mu m^2$ and with 100 ms dwell time per pixel. XRF signal was detected by an 80 $mm^2$ SDD detector. The incoming flux was monitored using a drilled photodiode and was used for normalization of the XRF elemental intensities. The XRF signals were energy-calibrated, and S elemental maps were obtained by fitting the XRF spectrum at each pixel using PyMCA software.[22] From the $\mu$-XRF S images spots were selected to perform $\mu$-XANES at the S k-


DOI: 10.1021/acs.cgd.8b01020
Cryst. Growth Des. 2018, 18, 5663−5673

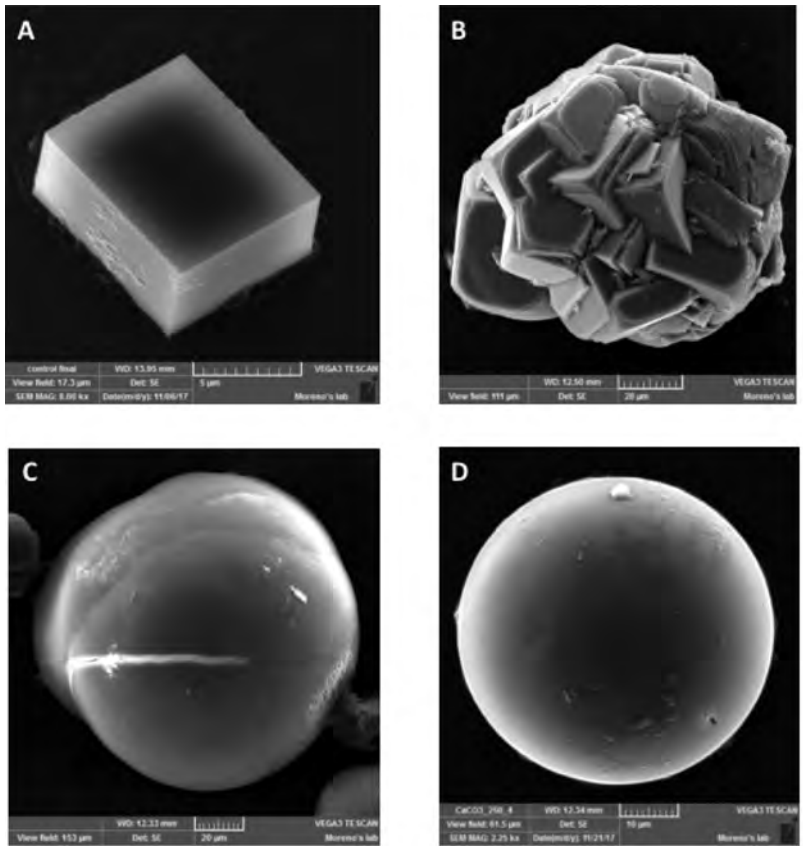


**Figure 4.** Effect of protein addition of CCA-1 from *C. acutus* respect to the control (A). The crystal growth of calcite in the presence of CCA-1: 100 (B), 250 (C), and 500 (D) $\mu$g/mL. The intramineral protein from the species of crocodile *C. acutus* produced spherical growth at concentrations higher than 250 $\mu$g/mL.

edge (2460−2500 eV, 0.5 eV energy steps). The obtained $\mu$-XANES spectra were processed using Athena[23] for pre-edge background subtraction and postedge normalization. The spectra from the samples was compared to references from L-cysteine and $ZnSO_4$ using multivariate statistical tools from the Orange data mining software.[24] First an unsupervised principal component analysis was performed on the data followed by cluster K-means. All this characterization was performed at the European Synchrotron Radiation Facility (beamline ID21, ESRF), Grenoble France.[25]

## 3. RESULTS AND DISCUSSION

**3.1. Biochemical Identification by Mass Spectroscopy and Gel Electrophoresis.** As we already stated, the eggshell from emu usually contains two intramineral proteins; these are called dromaiocalcins (DCAs). We even mentioned that eggshells of crocodiles also contain two proteins, and these are called crococalcins (CCAs). However, it is the dromaiocalcins that are difficult to separate, as they have similar contents of amino acids and show high similarity in molecular weight. The purification procedure was optimized to find the best-suited conditions. DCA-1, CCA-1 and DCA-2, CCA-2 were subsequently separated through gel permeation chromatography and by reverse-phase column. Mass spectroscopy was used to check the purity of these proteins based on their molecular weight as well as gel electrophoresis (Figure 2). Both DCA-1 and DCA-2 showed almost similar molecular weights, 16 333.6862 and 16 668.4401 Da, respectively. Similarly, the purification of CCA-1 and CCA-2 was also accomplished through gel permeation chromatography and reverse-phase chromatography. This purification was hard to perform, because the availability of eggshells from crocodiles are only at certain periods of the year. The purification yielded two main peaks that were collected separately. On the one hand, as it happened in the previous results, CCA-1 and CCA-2 showed again very similar molecular weights, 14 304.7179 and 14 620.6518 Da, respectively. On the other hand, isoelectric point determination for all these intramineral proteins agreed with that of the reported proteins, which participate in biomineralization processes;[20] it showed an acidic value. These acidic proteins seem to be determinant for the interaction with $CaCO_3$ as well as for the degree of phosphorylation of certain serines.[12,26,27]

From these results, the isoelectric points for DCA-1 and DCA-2 were 6.8 and 5.3, respectively. These values are in a good agreement with the reported values as already mentioned. However, for the particular case of CCA-1 and CCA-2 these isoelectric points were 5.2 and 5.9, respectively. In our previous publication we reported the high sensitivity for carbonate ions of these proteins.[17,28] It was also demonstrated for the intramineral proteins isolated from crocodiles by using dynamic light scattering and electroanalytical techniques like cyclic voltammetry. As it can be appreciated (see Figures S1−S3 in Supporting Information) DCA-1, DCA-2, CCA-1, and CCA-2 were selective for carbonate ions rather than sulfates and phosphates. However, cyclic voltammetry showed that particularly DCA-2 and CCA-2 were highly specific for carbonates compared to other proteins.

**3.2. The Effect of DCA-1, DCA-2, CCA-1, and CCA-2 on the Crystallization of Calcite.** We found some publications



DOI: 10.1021/acs.cgd.8b01020
*Cryst. Growth Des.* 2018, 18, 5663−5673

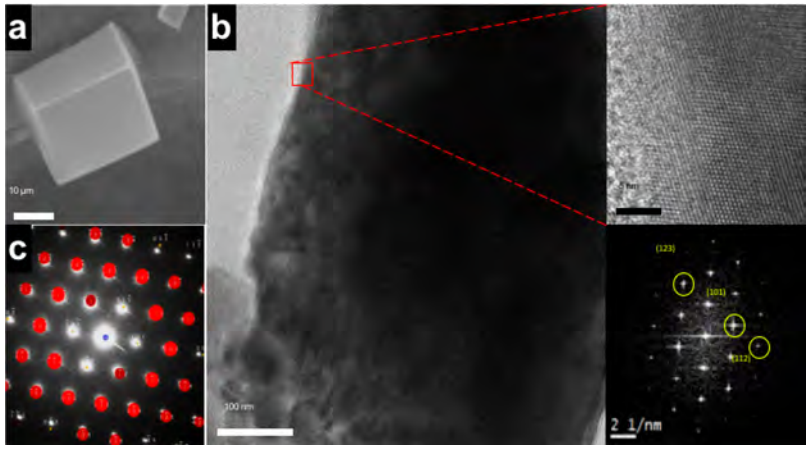


**Figure 5.** Electron microscopy characterization of the synthetically obtained calcite used as control. SEM reference image (a). TEM image of a single crystalline formation of $CaCO_3$ (b). (inset) High-resolution images and its respective Fourier transform showing reflections that correspond to the (101), (112), and (123) $CaCO_3$ planes. SAED pattern and matching for a rhombohedral crystal system (c).

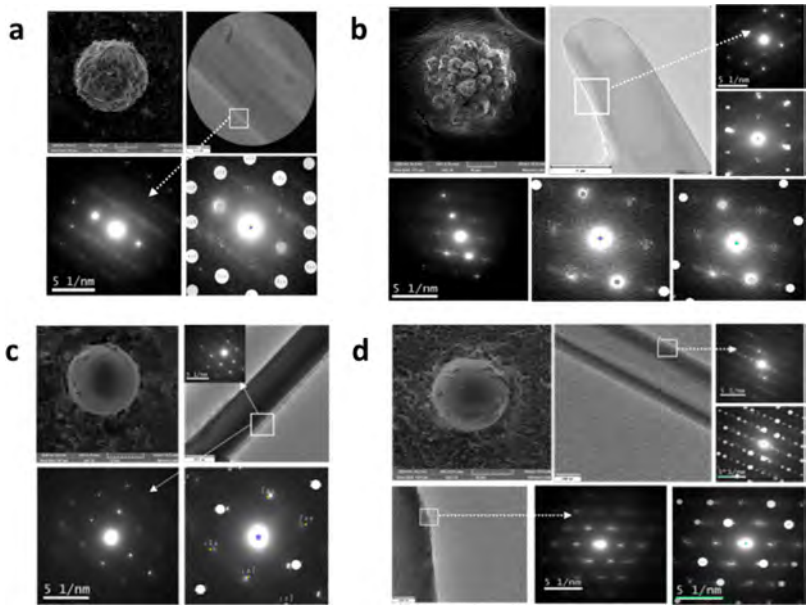


**Figure 6.** TEM characterization of (a) crystals of calcium carbonate with DCA-1, (b) calcium carbonate with DCA-2, (c) calcium carbonate with CCA-1, and (d) calcium carbonate with CCA-2.

that deal with to the use of protein matrix fractions on the crystallization of calcium carbonate,[29] but none involving proteins of crocodile's eggshells. Our study was performed using the experimental setup previously described in Figure 1. The crystallization of calcite (control without protein) usually takes place in ~3 d.

Here, we evaluated the influence of the intramineral proteins at 100, 250, or 500 μg/mL (DCA-1, DCA-2, CCA-1, and CCA-2) on the crystal growth of calcite. We found that the morphology of the crystals was affected as shown in Figure 3. Nonetheless, CCA-1 and CCA-2 affected significantly the morphology of these crystals. Finally, with CCA-1 and CCA-2, ellipsoidal and spherical-shaped crystals are obtained even with a lowest concentration of proteins.

From these results, clearly the influence of intramineral proteins from the crocodile (CCA-1 and CCA-2 from the species *C. moreletii*) on the crystal growth of calcite is rather remarkable. However, to have clarity whether the type of intramineral protein would have any influence depending on the type of crocodile, we decided to test a different crocodile from the Mexican species (*C. acutus*). Figure 4 shows this result, where we can appreciate that the two intramineral proteins produced spherical growth as well. The critical concentration was above 250 μg/mL; higher concentrations of this value produced spherical growth in both cases of intramineral proteins from crocodiles. There is no structural-based mechanism that could explain this crystal behavior; however, it can be related to the existence of the phosphorylated groups of the proteins, which could attract the calcium (2+) at the earlier stages of the crystallization.[12,26,27] This tendency was observed by using electroanalytical methods (see Supporting Information Figures S1–S3), where DCA-2 and CCA-2 were highly selective for carbonate ions. Most of the proteins of the group DCA-2, RCA-2 (not included in this study), and CCA-2 are usually facing post-translational modifications related to a phosphorylation of serine amino acids.



DOI: 10.1021/acs.cgd.8b01020
*Cryst. Growth Des.* 2018, 18, 5663–5673

The obtaining of rounded aggregates, based on our experiments, indicates that this adsorption is specific to certain faces. From our results we can infer that, at the beginning, aggregates are the first to be formed, whereas at the end, the transformation take place to a more stable form of calcium carbonate. Recent publications have suggested that certain polymorphs can be obtained under two main processes: (1) the one based on the classic nucleation theory, and (2) the one related to the formation of prenucleation clusters. If we consider this second process the presence of amorphous calcium carbonate is not excluded.[30] However, there are few available theoretical and computational simulations on the mechanism about these processes of interaction between protein and inorganic crystals.[31] On the one hand, currently, there is a contribution using molecular dynamics simulations applied to struthiocalcin-1 from ostrich eggshell taking the most important proteins to investigate the binding; it showed different domains binding the mineral surface of calcite.[32] On the other hand, when using a protein like lysozyme from the hen egg white, which is not intramineral, the effect on calcite faces and crystal habit modification is nonsignificant. This effect of lysozyme on the growth of calcite crystal only produced changes in the crystal size distribution but not any effect on changing the crystal habit.[28]

**3.3. Characterization by Electron Diffraction.** All crystals whether spherical- or rhombohedral-shaped were properly characterized by electron diffraction methods. These crystals were directly grown on TEM copper grids for further analysis.

This characterization proved that all controls for calcium carbonate crystallized in the polymorph calcite (Figure 5). Images taken at high-resolution transmission electron microscopy (HRTEM) show the crystalline structure of the synthesized control samples. Figure 6B shows an inset, which corresponds to the fast Fourier transform (FFT) and that corresponds to the crystal oriented along the ⟨111⟩ zone axis. Indexation indicates a rhombohedral $CaCO_3$ (calcite) crystalline phase. The spots measured in the FFT correspond to the planes (011), (112), and (123).

The influence of these proteins on the synthesis of calcium carbonate was based on the experimental setup of Figure 1 but using a TEM grid instead of using glass cover slides.[14] The presence of DCA-1 isolated from the eggshells of emu (*D. novahollandiae*) showed the obtaining of the polymorph calcite according to the electron diffraction patterns (Figure 6a). For the particular case of DCA-2, the electron diffraction pattern was a mixture between calcite and vaterite (Figure 6b). We can say that both proteins DCA-1 and DCA-2 can induce in general the formation of calcite in the eggshell, but one of those DCA-1, which is more abundant, influences specifically the obtaining of calcite in a higher proportion. Nonetheless, the influence of intramineral proteins from crocodile (*C. moreletii*) upon the synthesis of calcium carbonate was as follows: either CCA-1 (Figure 6c) or the protein CCA-2 (Figure 6d) lead the obtaining of the polymorph aragonite only. In nature both polymorphs calcite and aragonite are the most common polymorphs in different eggshells of animals (birds, reptiles, and amphibian) even in mineralized parts of marine organisms; sometimes the synthesis of calcite or aragonite depends on the environment (Table 1).[33]

Additionally, we compared transversal sections SEM micrographs of eggshells of four types of species (Figure 7). We took hen eggshell (as reference), emu, crocodile, and an eggshell of a dinosaur (70 million years old, donated by the department of Geology of the National Autonomous University of Mexico). The dinosaur was originally found in the Rosario area in Baja California, Mexico, in the Gallo formation. Different areas of the eggshells were compared to observe how the transversal cut looks and to characterize that via X-ray absorption.

**Table 1. Synthesis of Calcium Carbonate and the Type of Obtained Polymorph, When Interacting with Intramineral Proteins**

| $CaCl_2 + (NH_4)_2CO_3 \rightarrow CaCO_3 + NH_4Cl$ | DCA-1 | DCA-2 | CCA-1 | CCA-2 |
|---|---|---|---|---|
| type of polymorph | calcite | calcite/vaterite | aragonite | aragonite |

From these micrographs it can be appreciated that even for the mineralized part of the hadrosauridae the four zones are still preserved. The mammillary cones show that along 70 million years this part seems to be much more homogeneous area; perhaps it solidified as a single crystal of calcite due to diffusion processes. Some remarkable differences are observed in the cuticle zone and in the mammillary cones area.

**3.4. Identification of Proteins by LC-MS/MS and Alignment of Multiple Sequences.** We performed the identification of the proteins CCA-1 and CCA-2 from *C. moreletti*, since the sequence of these two proteins is not yet available. A series of sequence fragments was identified, and the fragments were compared with those intramineral proteins already sequenced and published (SCA-1, SCA-2, DCA-1, DCA-2, RCA-1, and RCA-2). The fragments obtained for CCA-1 are shown in Table 2. It can be appreciated that fragments of CCA-1 are homologous to the proteins DCA-1, SCA-1, and RCA-1. Nevertheless, as the fragments of CCA-2 are concerned, we did not find any homology with the intramineral proteins already reported. This does not mean that CCA-2 is different, it simply means that the identification method was not powerful enough to collect the right fragments. Additionally, the amount of CCA-2 in the eggshell is a limiting factor.

To know the percentage of similarity with the reported intramineral proteins with a C-type lectin domain (CTLD) in the eggshell, we performed a multiple sequencing alignment. The birds of the superorder Palaeognathae (*S. camelus*, *R. americana*, and *D. novaehollandiae*) in comparison with *G. gallus* presented a 36−44% of identity. At the same time, in the same superorder the proteins were divided into two main groups. The type I corresponds to proteins with a 69.70% of identity like SCA-1 and DCA-1, 73.48% between SCA-1 and RCA-1 and 77.04% for DCA-1 and RCA-1. Type two corresponds to SCA-2 and DCA-2 with 82.98%, SCA-2 with RCA-2 with 78.45%, and finally DCA-1 and RCA-2 with 78.17%.

**3.5. Analysis of Eggshells by X-ray Absorption Near-Edge Structure and X-ray Fluorescence Spectroscopy.** We combined $\mu$-XRF and $\mu$-XANES of the ID21 X-ray beamline facilities at the ESRF (Grenoble, France) as a very powerful strategy that consisted of scanning each point (pixel) of the whole sample at fixed incident energy and collected a fluorescence spectrum.[25] On the basis of the $\mu$-XRF images, all selected points of interest were spectroscopically analyzed by $\mu$-XANES as shown in Figure 8 for the analysis of eggshells from emu and dinosaur eggshells donated by the Institute of Geology UNAM (the samples were collected in the Northern



DOI: 10.1021/acs.cgd.8b01020
Cryst. Growth Des. 2018, 18, 5663−5673

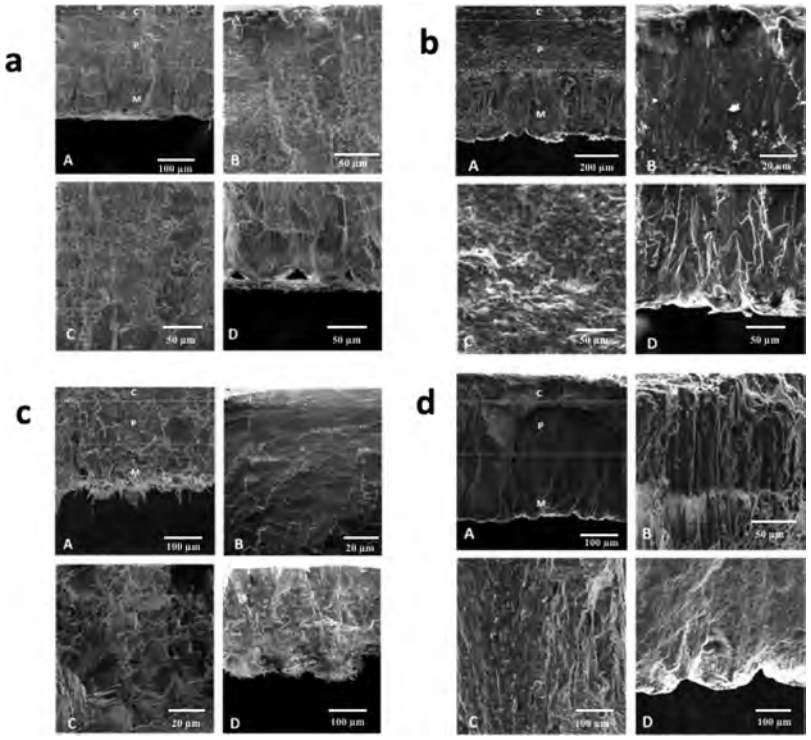


**Figure 7.** Transversal SEM micrographs of four types of eggshells: (a) *G. gallus*, (b) *D. novahollandiae*, (c) *C. moreletii*, and (d) *Hadrosauridae* of 70 million years old. Each section represents (A) general overview of the eggshell, (B) cuticle, (C) mammillary palisade, and (D) enlarged view of mammillary cones.

**Table 2. Alignment and Comparison of Sequences for Crococalcins and Similarity with Those Proteins from Ostrich and Emu**

| protein | obtained peptides (fragments) | homologous proteins |
|---|---|---|
| CCA-1 | FVSQCQRGEEEENVWIGLR | DCA-1 |
| | ALRDGCHLASIHSAEEHR | SCA-1 |
| | LWAWSDGSK | RCA-1 |
| | GNCYGYFR | |
| CCA-2 | EGPFKKLFGR | not detected |

part of Mexico in Rosario Baja California in the Gallo formation).

The analyses of the eggshells were focused in three areas along the layer from the bottom to the upper part of the calcified layer (from mammillary cones up to the end of the palisade). This scanning in different areas was performed to estimate the distribution of organic sulfur along the sample.

In the case of crocodiles, the eggshell is thinner than that of the emu, and $\mu$-XANES analyses were performed only on inside and outside layers. All the $\mu$-XANES spectra from samples and references were submitted to multivariate statistical analysis. Figure 9 shows the scatter plot of principal component 1 (PC1) versus PC2 and cluster density obtained by k-means. The results showed clustering around the L-cysteine (-SH) reference compound for all the spectra obtained from dinosaur, the crocodile inner shell, and almost all spectra from emu. Cluster C1 is composed by crocodile external shell and E2 spectra from emu, whereas the sulfate reference spectrum is alone in C2. The applied analysis confirms the spectral similarity of the S species in modern eggshells and the fossil samples. The similarity is due to the presence of absorption signals at 2473.4 eV characteristic of S−S/SH organic bonds as in L-cysteine. The C1 cluster differs in the contribution from $SO_4^{-2}$ in the external shell of crocodile and the mineralized region from emu.

It is important to remark that all samples were perfectly cleaned to avoid any contaminants. The presence of organic sulfur as that corresponding to L-cysteine opens the possibility of having encapsulated proteins (or remaining peptides of a very old protein) perhaps preserved for a long time in the mineral part. This is a plausible approach, as it has been recently applied to obtain ancestral proteins. The scientist resurrected an ancestral protein (Precambrian $\beta$-lactamase) based on models of sequence evolution.[34]

Additionally, in our case to demonstrate whether the mineral phase is preserved in the dinosaur eggshell, we exposed a piece of dinosaur eggshell to acetic acid (1 M) hoping that if there was calcite in the mineral part of the eggshell, bubbles of $CO_2$ would be expelled, and that was exactly what happened. We included in the Supporting Information a short video showing this process. The presence of acetic acid produces bubbles of $CO_2$ when interacting with the mineral part of calcite of the dinosaur eggshell.

On the basis of this approach, our next goal will be the isolation and purification of these intramineral biomolecules from the eggshells of the dinosaur, which are probably encapsulated into the eggshell structure protected by mineralized layer for almost 70 million years as shown by the $\mu$-XANES and $\mu$-XRF investigations. Recently, Demarchi et al. (2016) made an investigation on archeological dig discovery preserved fossil proteins in ostrich eggshells that were 3.8 billion years old.[35] They analyzed ostrich eggshells from Tanzania and South Africa. Their computerized models showed that the proteins survived the harsh conditions due to mineral bonding within the shell. The proteins that were



DOI: 10.1021/acs.cgd.8b01020
Cryst. Growth Des. 2018, 18, 5663−5673

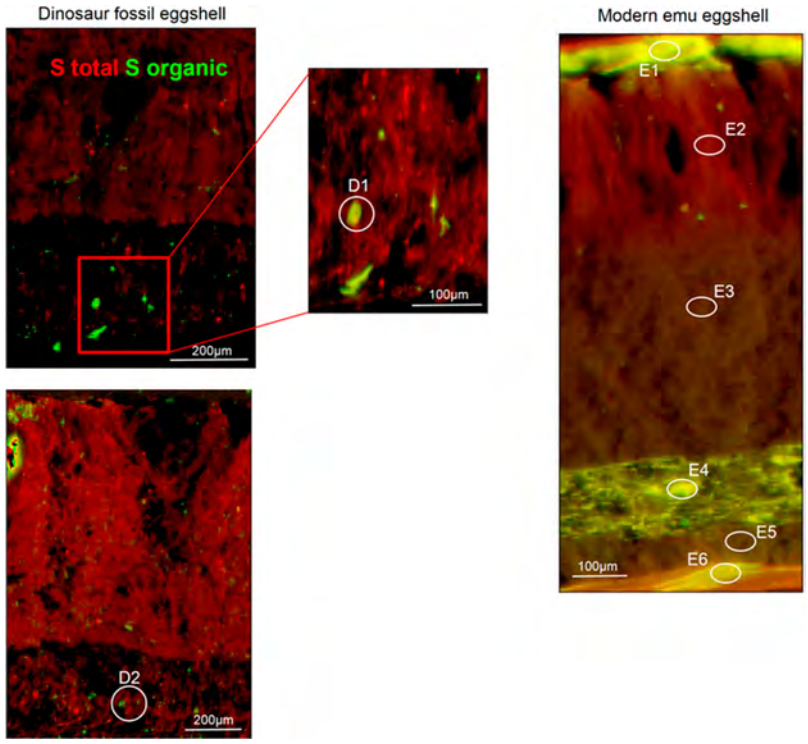


**Figure 8.** $\mu$-XRF maps of S species taken at 2437.4 eV (organic S−S/SH) and 2500 eV (total S content). Regions marked as D1 and D2 correspond to $\mu$-XANES spectra of the fossil dinosaur samples and E1−E6 for the modern emu.

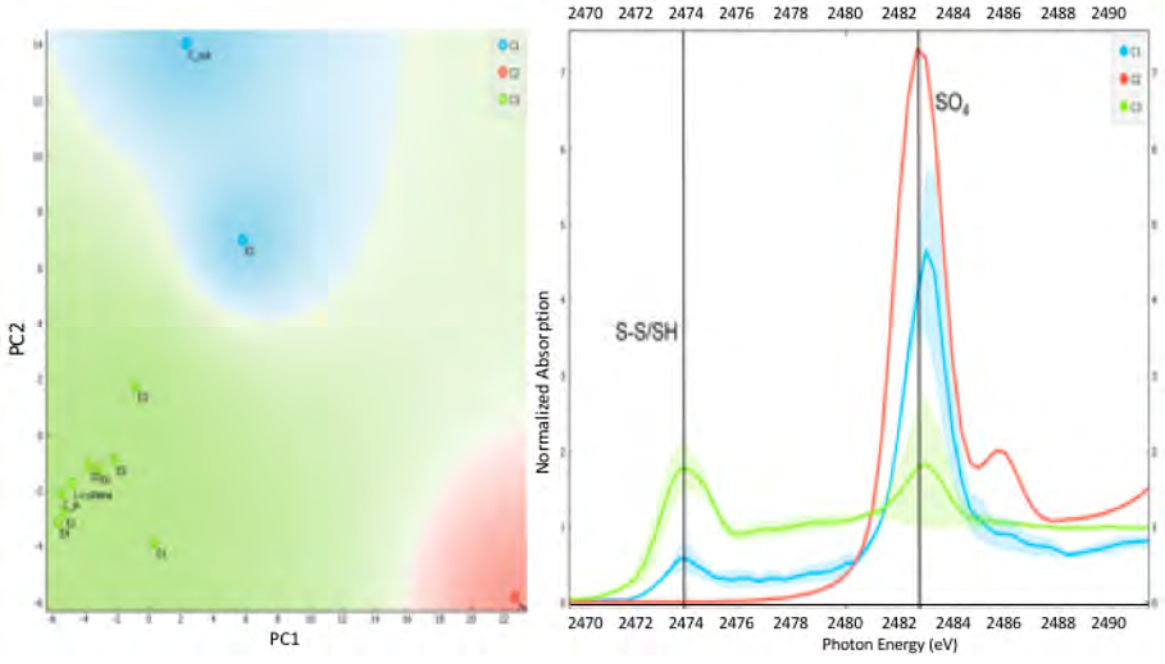


**Figure 9.** PCA scatter plot (PC1vs PC2) of $\mu$-XANES spectra from the eggshell samples, L-cysteine, and $ZnSO_4$ (left). Average XANES spectra (±standard deviation) for members of the three clusters obtained by k-means (right). Emu (E1-E6), crocodile (C_in and C_out), and fossil dinosaur (D1 and D2). Lines represent the average position for thiol/disulfide organic bonds (2473.4 eV) and sulfate (2482.6 eV).

partially isolated (Struthiocalcin-1, SCA-1) could be compared with our published results[11] on the crystal structure of SCA-1 finding a very high similarity.

Our results will open the possibility of having a real protein from the eggshell of a dinosaur (or fractions of that ancient biological macromolecule) that could be isolated and released after a long time of encapsulation via mineralization processes. This research will contribute to the recent coined area of research called Paleoproteomics, where ancient proteins may be resurrected.[36] We demonstrated along with this contribution that the proteins of emu and crocodiles are phylogenetically related, and if the intramineral proteins of the dinosaur eggshell are isolated, we will probably be able to demonstrate that these ancient proteins are phylogenetically similar. We can



DOI: 10.1021/acs.cgd.8b01020
Cryst. Growth Des. 2018, 18, 5663−5673

assume that there is a great opportunity to have those proteins still safe or intact, as our synchrotron $\mu$-XRF/$\mu$-XANES investigations have shown.

## 4. CONCLUSIONS

By means of electroanalytical methods, it was determined that proteins CCA-1 and CCA-2 have a high selectivity for carbonate ions as well as those proteins isolated from emu (DCA-1 and DCA-2). The crystal growth of calcite and modification of the shape due to intramineral proteins, turning this into spherical crystal growth of calcium carbonate polymorphs, can have important implications into the mineralization processes. The sphere's formation could be associated with the presence of phosphorylated groups of the protein with negative charges that perhaps interact with calcium ions at the very early stages of crystallization processes. This trend was more remarkable when using the proteins isolated from the crocodile eggshells (CCA-1 and CCA-2). We could infer that these proteins contain a higher number of phosphorylated groups than those obtained in the intramineral proteins of emu.

Finally, X-ray absorption techniques like XANES as well as XRF demonstrated that there is a possibility of having a small amount of protein fractions still preserved into the dinosaur eggshell of 70 million years old. There is a high probability to find ancestral proteins in the dinosaur eggshell to be compared with those intramineral proteins found in the eggshells of ratite birds.

## ■ ASSOCIATED CONTENT

### Supporting Information

The Supporting Information is available free of charge on the ACS Publications website at DOI: 10.1021/acs.cgd.8b01020.

Analysis of conformational stability through dynamic light scattering. Analysis of the interaction of proteins with carbonate ions through cyclic voltammetry (PDF)

### Web-Enhanced Feature

A short video showing a piece of dinosaur eggshell exposed to acetic acid (1 M) expelling bubbles of $CO_2$ demonstrating that calcite layer forming the mineral part of the dinosaur's eggshell was preserved a long time.

## ■ AUTHOR INFORMATION


### Corresponding Author

*E-mail: carcamo@unam.mx.

### ORCID

Abel Moreno: 0000-0002-5810-078X


### Author Contributions

A.L.F. isolated, purified, and characterized the proteins from emu and one species of crocodile (*C. moreletii*). Additionally she performed the crystallization of calcite in the presence of intramineral proteins; A.D.-T. as well as O.V.G. isolated, purified, and characterized the second species of crocodile (*C. acutus*); E.O. and A.P. performed transmission electron microscopy and electron diffraction analysis; H.C.M. performed the $\mu$-XRF and $\mu$-XANES analyses on the eggshells reported; J.P.R.G. performed the protein identification by mass spectroscopy; R.H.-R. supplied the dinosaur eggshell as well as the identification and location of the nest in the northern part of Mexico; M.C.C. performed the sequencing and identification of the proteins from the crocodile eggshells; and A.M. conceived and designed this contribution as well as coordinated the writing and contents of this manuscript. This contribution was written through the contribution of all authors. All authors agreed to the final version of this manuscript already revised.

### Notes

The authors declare no competing financial interest.

## ■ ACKNOWLEDGMENTS


A.N.L.-F. thanks CONACYT (registration No. 385795) for the scholarship for the MSc studies in the Graduate Program in Biological Sciences of Univ. Nacional Autónoma de México. One of the authors (A.M.) acknowledges the support from DGAPA-UNAM, PAPIIT Project No. IG200218. R.H.-R. acknowledges PAPIIT Project No. IN 130316. The TEM work was performed in the Kleberg Advanced Microscopy Center and supported by the National Institute on Minority Health and Health Disparities (G12MD007591) from the NIH. We acknowledge the beamtime granted at beamline ID21 of the ESRF for this research. This is a research of scientists from the network REDTULS-CONACYT that uses synchrotron facilities for applications to biological sciences.


## ■ REFERENCES


(1) Cuellar-Cruz, M. Synthesis of inorganic and organic crystals mediated by proteins in different biological organisms. A mechanism of biomineralization conserved throughout evolution in all living species. *Prog. Cryst. Growth Charact. Mater.* **2017**, *63*, 94−103.

(2) Roberts, A. P. Magnetic mineral diagenesis. *Earth-Sci. Rev.* **2015**, *151*, 1−47.

(3) Webb, J.; Macey, D. J.; Chua-anusorn, W.; St Pierre, T. G.; Brooker, L. R.; Rahman, I.; Noller, B. Iron biominerals in medicine and the environment. *Coord. Chem. Rev.* **1999**, *190*, 1199−1215.

(4) Yao, S. S.; Jin, B. A.; Liu, Z. M.; Shao, C. Y.; Zhao, R. B.; Wang, X. Y.; Tang, R. K. Biomineralization: From Material Tactics to Biological Strategy. *Adv. Mater.* **2017**, *29*, 1605903.

(5) Prasad Shastri, V. Biomineralization: A confluence of materials science, biophysics, proteomics, and evolutionary biology. *MRS Bull.* **2015**, *40* (6), 473−477.

(6) Sahni, A. Biomineralization: Some complex crystallite-oriented skeletal structures. *J. Biosci.* **2013**, *38*, 925−935.

(7) Rose-Martel, M.; Smiley, S.; Hincke, M. T. Novel identification of matrix proteins involved in calcitic biomineralization. *J. Proteomics* **2015**, *116*, 81−96.

(8) Rodriguez-Navarro, A. B.; Marie, P.; Nys, Y.; Hincke, M. T.; Gautron, J. Amorphous calcium carbonate controls avian eggshell mineralization: A new paradigm for understanding rapid eggshell calcification. *J. Struct. Biol.* **2015**, *190*, 291−303.

(9) Reyes-Grajeda, J. P.; Moreno, A.; Romero, A. Crystal structure of ovocleidin-17, a major protein of the calcified Gallus gallus eggshell - Implications in the calcite mineral growth pattern. *J. Biol. Chem.* **2004**, *279*, 40876−40881.

(10) Reyes-Grajeda, J. P.; Marin-Garcia, L.; Stojanoff, V.; Moreno, A. Purification, crystallization and preliminary X-ray analysis of struthiocalcin 1 from ostrich (Struthio camelus) eggshell. *Acta Crystallogr., Sect. F: Struct. Biol. Cryst. Commun.* **2007**, *63*, 987−989.

(11) Ruiz-Arellano, R. R.; Medrano, F. J.; Moreno, A.; Romero, A. Structure of struthiocalcin-1, an intramineral protein from Struthio camelus eggshell, in two crystal forms. *Acta Crystallogr., Sect. D: Biol. Crystallogr.* **2015**, *71*, 809−818.

(12) Mann, K.; Siedler, F. Amino acid sequences and phosphorylation sites of emu and rhea eggshell C-type lectin-like proteins. *Comp. Biochem. Physiol., Part B: Biochem. Mol. Biol.* **2006**, *143*, 160−170.

(13) Mann, K.; Siedler, F. Ostrich (Struthio camelus) eggshell matrix contains two different C-type lectin-like proteins. Isolation,




DOI: 10.1021/acs.cgd.8b01020
*Cryst. Growth Des.* 2018, 18, 5663−5673

amino acid sequence, and posttranslational modifications. *Biochim. Biophys. Acta, Proteins Proteomics* **2004**, *1696*, 41−50.
(14) Gomez-Morales, J.; Hernandez-Hernandez, A.; Sazaki, G.; Garcia-Ruiz, J. M. Nucleation and Polymorphism of Calcium Carbonate by a Vapor Diffusion Sitting Drop Crystallization Technique. *Cryst. Growth Des.* **2010**, *10*, 963−969.
(15) Castillo-Michel, H. A.; Diaz-Sanchez, A. G.; Martinez-Martinez, A.; Hesse, B. Investigations of Sulfur Chemical Status with Synchrotron Micro Focused X-ray fluorescence and X-ray Absorption Spectroscopy. *Protein Pept. Lett.* **2016**, *23*, 291−299.
(16) Cusack, M.; Dauphin, Y.; Cuif, J. P.; Salome, M.; Freer, A.; Yin, H. Micro-XANES mapping of sulphur and its association with magnesium and phosphorus in the shell of the brachiopod, Terebratulina retusa. *Chem. Geol.* **2008**, *253*, 172−179.
(17) Ruiz-Arellano, R. R.; Moreno, A. Obtainment of Spherical-Shaped Calcite Crystals Induced by Intramineral Proteins Isolated from Eggshells of Ostrich and Emu. *Cryst. Growth Des.* **2014**, *14*, 5137−5143.
(18) Virgen-Ortiz, J. J.; Ibarra-Junquera, V.; Osuna-Castro, J. A.; Escalante-Minakata, P.; Mancilla-Margalli, N. A.; Ornelas-Paz, J. D. Method to concentrate protein solutions based on dialysis-freezing-centrifugation: Enzyme applications. *Anal. Biochem.* **2012**, *426*, 4−12.
(19) Lapinska, U.; Saar, K. L.; Yates, E. V.; Herling, T. W.; Muller, T.; Challa, P. K.; Dobson, C. M.; Knowles, T. P. J. Gradient-free determination of isoelectric points of proteins on chip. *Phys. Chem. Chem. Phys.* **2017**, *19*, 23060−23067.
(20) Hernandez-Hernandez, A.; Rodriguez-Navarro, A. B.; Gomez-Morales, J.; Jimenez-Lopez, C.; Nys, Y.; Garcia-Ruiz, J. M. Influence of model globular proteins with different isoelectric points on the precipitation of calcium carbonate. *Cryst. Growth Des.* **2008**, *8*, 1495−1502.
(21) Stadelmann, P. A. Ems - a Software Package for Electron-Diffraction Analysis and Hrem Image Simulation in Materials Science. *Ultramicroscopy* **1987**, *21*, 131−145.
(22) Sole, V. A.; Papillon, E.; Cotte, M.; Walter, P.; Susini, J. A multiplatform code for the analysis of energy-dispersive X-ray fluorescence spectra. *Spectrochim. Acta, Part B* **2007**, *62*, 63−68.
(23) Ravel, B.; Newville, M. ATHENA, ARTEMIS, HEPHAESTUS: data analysis for X-ray absorption spectroscopy using IFEFFIT. *J. Synchrotron Radiat.* **2005**, *12*, 537−541.
(24) Demsar, J.; Curk, T.; Erjavec, A.; Gorup, C.; Hocevar, T.; Milutinovic, M.; Mozina, M.; Polajnar, M.; Toplak, M.; Staric, A.; Stajdohar, M.; Umek, L.; Zagar, L.; Zbontar, J.; Zitnik, M.; Zupan, B. Orange: Data Mining Toolbox in Python. *J. Mach Learn Res.* **2013**, *14*, 2349−2353.
(25) Cotte, M.; Pouyet, E.; Salome, M.; Rivard, C.; De Nolf, W.; Castillo-Michel, H.; Fabris, T.; Monico, L.; Janssens, K.; Wang, T.; Sciau, P.; Verger, L.; Cormier, L.; Dargaud, O.; Brun, E.; Bugnazet, D.; Fayard, B.; Hesse, B.; Pradas Del Real, A. E.; Veronesi, G.; Langlois, J.; Balcar, N.; Vandenberghe, Y.; Sole, V. A.; Kieffer, J.; Barrett, R.; Cohen, C.; Cornu, C.; Baker, R.; Gagliardini, E.; Papillon, E.; Susini, J. The ID21 X-ray and infrared microscopy beamline at the ESRF: status and recent applications to artistic materials. *J. Anal. At. Spectrom.* **2017**, *32*, 477−493.
(26) Hecker, A.; Testeniere, O.; Marin, F.; Luquet, G. Phosphorylation of serine residues is fundamental for the calcium-binding ability of Orchestin, a soluble matrix protein from crustacean calcium storage structures. *FEBS Lett.* **2003**, *535*, 49−54.
(27) Mann, K.; Olsen, J. V.; Macek, B.; Gnad, F.; Mann, M. Phosphoproteins of the chicken eggshell calcified layer. *Proteomics* **2007**, *7*, 106−115.
(28) Marin-Garcia, L.; Frontana-Uribe, B. A.; Stojanoff, V.; Serrano-Posada, H. J.; Moreno, A. Chemical recognition of carbonate anions by proteins involved in biomineralization processes and their influence on calcite crystal growth. *Cryst. Growth Des.* **2008**, *8*, 1340−1345.
(29) Hernandez-Hernandez, A.; Vidal, M. L.; Gomez-Morales, J.; Rodriguez-Navarro, A. B.; Labas, V.; Gautron, J.; Nys, Y.; Garcia Ruiz, J. M. Influence of eggshell matrix proteins on the precipitation of calcium carbonate (CaCO3). *J. Cryst. Growth* **2008**, *310*, 1754−1759.
(30) Gebauer, D.; Kellermeier, M.; Gale, J. D.; Bergstrom, L.; Colfen, H. Pre-nucleation clusters as solute precursors in crystallisation. *Chem. Soc. Rev.* **2014**, *43*, 2348−2371.
(31) Sun, W. H.; Ceder, G. Induction time of a polymorphic transformation. *CrystEngComm* **2017**, *19*, 4576−4585.
(32) Xue, Z. Y.; Shen, Q. Y.; Liang, L. J.; Shen, J. W.; Wang, Q. Adsorption Behavior and Mechanism of SCA-1 on a Calcite Surface: A Molecular Dynamics Study. *Langmuir* **2017**, *33*, 11321−11331.
(33) Feng, Q. L.; Pu, G.; Pei, Y.; Cui, F. Z.; Li, H. D.; Kim, T. N. Polymorph and morphology of calcium carbonate crystals induced by proteins extracted from mollusk shell. *J. Cryst. Growth* **2000**, *216*, 459−465.
(34) Risso, V. A.; Gavira, J. A.; Mejia-Carmona, D. F.; Gaucher, E. A.; Sanchez-Ruiz, J. M. Hyperstability and Substrate Promiscuity in Laboratory Resurrections of Precambrian beta-Lactamases (vol 135, pg 2899, 2013). *J. Am. Chem. Soc.* **2013**, *135*, 10580−10580.
(35) Demarchi, B.; Hall, S.; Roncal-Herrero, T.; Freeman, C. L.; Woolley, J.; Crisp, M. K.; Wilson, J.; Fotakis, A.; Fischer, R.; Kessler, B. M.; Jersie-Christensens, R. R.; Olsen, J. V.; Haile, J.; Thomas, J.; Marean, C. W.; Parkington, J.; Presslee, S.; Lee-Thorp, J.; Ditchfield, P.; Hamilton, J. F.; Ward, M. W.; Wang, C. M.; Shaw, M. D.; Harrison, T.; Dominguez-Rodrigo, M.; MacPheel, R. D. E.; Kwekason, A.; Ecker, M.; Horwitz, L. K.; Chazan, M.; Kroger, R.; Thomas-Oates, J.; Harding, J. H.; Cappellini, E.; Penkman, K.; Collins, M. J. Protein sequences bound to mineral surfaces persist into deep time. *eLIFE* **2016**, *5*, 1.
(36) Hendy, J.; Welker, F.; Demarchi, B.; Speller, C.; Warinner, C.; Collins, M. J. A guide to ancient protein studies. *Nat. Ecol Evol* **2018**, *2*, 791−799.


DOI: 10.1021/acs.cgd.8b01020
*Cryst. Growth Des.* 2018, 18, 5663−5673